

# Stable isotope signatures in historic harbor seal bone link food web-assimilated carbon and nitrogen resources to a century of environmental change

Megan L. Feddern<sup>1</sup>  | Gordon W. Holtgrieve<sup>1</sup>  | Eric J. Ward<sup>2</sup> 

<sup>1</sup>School of Aquatic and Fishery Sciences, University of Washington, Seattle, WA, USA

<sup>2</sup>Conservation Biology Division, Northwest Fisheries Science Center, National Marine Fisheries Service, Seattle, WA, USA

## Correspondence

Megan L. Feddern, School of Aquatic and Fishery Sciences, University of Washington, 1122 NE Boat Street, Seattle, WA 98105, USA.

Email: mfeddern@uw.edu

## Funding information

Washington Sea Grant, University of Washington, Grant/Award Number: NA18OAR4170095 and NA19OAR4170360; Joint Institute for the Study of the Atmosphere and Ocean, Grant/Award Number: 2020-1116

## Abstract

Anthropogenic climate change will impact nutrient cycles, primary production, and ecosystem structure in the world's oceans, although considerable uncertainty exists regarding the magnitude and spatial variability of these changes. Understanding how regional-scale ocean conditions control nutrient availability and ultimately nutrient assimilation into food webs will inform how marine resources will change in response to climate. To evaluate how ocean conditions influence the assimilation of nitrogen and carbon into coastal marine food webs, we applied a novel dimension reduction analysis to a century of newly acquired molecular isotope data derived from historic harbor seal bone specimens. By measuring bulk  $\delta^{13}\text{C}$  and  $\delta^{15}\text{N}$  values of source amino acids of these top predators from 1928 to 2014, we derive indices of primary production and nitrogen resources that are assimilated into food webs. We determined coastal food webs responded to climate regimes, coastal upwelling, and freshwater discharge, yet the strength of responses to individual drivers varied across the northeast Pacific. Indices of primary production and nitrogen availability in the Gulf of Alaska were dependent on regional climate indices (i.e., North Pacific Gyre Oscillation) and upwelling. In contrast, the coastal Washington and Salish Sea food webs were associated with local indices of freshwater discharge. For some regions (eastern Bering Sea, northern Gulf of Alaska) food web-assimilated production was coupled with nitrogen sources; however, other regions demonstrated no production-nitrogen coupling (Salish Sea). Temporal patterns of environmental indices and isotopic data from Washington state varied about the long-term mean with no directional trend. Data from the Gulf of Alaska, however, showed below average harbor seal  $\delta^{13}\text{C}$  values and above average ocean conditions since 1975, indicating a change in primary production in recent decades. Altogether, these findings demonstrate stable isotope data can provide useful indices of nitrogen resources and phytoplankton dynamics specific to what is assimilated by food webs.

## KEYWORDS

amino acid, climate change, compound-specific stable isotope analysis, Gulf of Alaska, harbor seals, northeast Pacific Ocean, primary production

## 1 | INTRODUCTION

Changing ocean conditions are reshaping the structure and function of marine food webs on regional scales. Ocean temperature (Hoegh-Guldberg & Bruno, 2010), oxygen availability (Briertburg et al., 2018), and climatic regimes such as El Niño Southern Oscillation (Vecchi & Wittenberg, 2010) alter nutrient availability and cycling, and thus, the ecological structure of marine systems. Projected global redistribution of nutrients suggests net primary production in the ocean is likely to change both spatially and temporally. Yet, substantial uncertainty remains, with predictions suggesting both increases and decreases in global net primary productivity of up to 20% by 2100 (Bopp et al., 2013; Gregg et al., 2003; Kwiatkowski et al., 2017). An important contributor to this uncertainty is regional variability in phytoplankton response to ocean conditions and how that variability will impact other trophic levels and dependent fisheries (Brander, 2010; Moore et al. 2018). Ocean conditions (i.e., sea surface temperature [SST], freshwater discharge, wind, and ice cover) have been associated with abundance and recruitment of many fish species in the Northeast Pacific (Cunningham et al., 2018; Puerta et al., 2019; Stachura et al., 2014). Nonetheless, these studies rarely include indicators of nutrient availability or primary production linking the ecosystem response to its environment. Understanding how regional and local scale physical drivers control nutrient availability and ultimately nutrient assimilation into food webs will be important for predicting the future availability of marine resources.

A strong empirical understanding of food web response to changing ocean conditions and nutrient constraints requires time series data that span multiple climate regimes to decouple natural variability with long-term anthropogenic changes. Currently, quantitative methods are also limited in their ability to scale primary production trends to ecosystem-level responses (Bonan & Doney, 2018). Stable isotope measurement of  $\delta^{15}\text{N}$  ( $^{15}\text{N}/^{14}\text{N}$ ) of individual amino acids is an emerging tool for reconstructing trends in nitrogen sources from historic specimens (McMahon et al., 2019; Sherwood et al., 2011, 2014; Whitney et al., 2019). The  $\delta^{15}\text{N}$  signature at the base of the food web is primarily controlled by utilization and the isotopic signatures of different nitrogen sources, particularly urea, nitrate, and ammonium, by primary producers (Graham et al., 2010; Ohkouchi et al., 2017). Measurements of bulk  $\delta^{15}\text{N}$  values from consumers can be difficult to attribute to changes at the base of the food web because trophic level shifts also effect the isotopic composition of bulk nitrogen (Fry, 2006). Amino acid-specific  $\delta^{15}\text{N}$  data address this challenge, as amino acids exhibit two distinct patterns in isotopic enrichment: trophic amino acids (i.e., glutamic acid, alanine, proline) become enriched in  $^{15}\text{N}$  with each trophic transfer and source amino acids (i.e., phenylalanine, lysine, methionine) show minimal change and thus are reflective of the base of the food web (Chikaraishi et al., 2009; McClelland & Montoya, 2002; Ohkouchi et al., 2017).

Similar to the nitrogen stable isotope composition of amino acids as a proxy for nitrogen sources, carbon isotopic composition has emerged as a useful tool for assessing historic changes in phytoplankton (Larsen et al., 2013; Lorrain et al., 2019; McMahon et al.,

2015). However, cellular growth rates, phytoplankton community composition, the isotopic composition of carbon in  $\text{CO}_2$ , and  $\text{CO}_2$  concentration all affect the  $\delta^{13}\text{C}$  ( $^{13}\text{C}/^{12}\text{C}$ ) values of phytoplankton in tandem (Burkhardt et al., 1999; Lorrain et al., 2019). The relative effects of these factors remain difficult to discern from carbon isotope data alone. Nonetheless, carbon stable isotope data are highly correlated with copepod biomass in the northeast Pacific and thus can be a useful combined index of ocean productivity (Espinasse et al., 2020). While both source amino acid  $\delta^{15}\text{N}$  and bulk  $\delta^{13}\text{C}$  values can be influenced by a number of biogeochemical and physiological processes (Figure 1), they are useful indicators of nitrogen utilization (source amino acid  $\delta^{15}\text{N}$ ) and phytoplankton dynamics (bulk  $\delta^{13}\text{C}$ ), despite the difficulty in identifying specific mechanisms of fractionation.

Here we use source amino acid  $\delta^{15}\text{N}$  and bulk  $\delta^{13}\text{C}$  values of consumer bone collagen as indicators of change in food web-assimilated nitrogen (nitrogen utilization and isotopic composition at the base of the food web) and food web-assimilated production (phytoplankton composition,  $[\text{CO}_2]$ , cellular growth, and physiology). These definitions assume major changes in nitrogen utilization and phytoplankton dynamics are recorded in the stable isotope composition of nitrogen and carbon in phytoplankton (de la Vega et al., 2020; McMahon et al., 2019; Ohkouchi et al., 2017; Sherwood et al., 2011), scaled to the spatial and temporal resource use of consumers, and conserved with minimal trophic fractionation (Chikaraishi et al., 2009). Bulk  $\delta^{13}\text{C}$  and  $\delta^{15}\text{N}$  values of source amino acids such as phenylalanine ( $\delta^{15}\text{N}_{\text{Phe}}$ ) from long-lived, generalist consumers provide ecosystem-level information of carbon and nitrogen dynamics that are integrated over space, time, and multiple energy pathways in the food web (de la Vega et al., 2020; McCann et al., 2005; Rooney et al., 2006). As a result, these data sources are more relevant to questions of food web responses to large-scale environmental forcing than discrete measurements of inorganic nutrients or phytoplankton. Ultimately these data can be used to understand how ecosystems have responded to environmental variability in the past and glean insights into food web responses to oceanic conditions in the future.

Harbor seals (*Phoca vitulina*) are a particularly well-suited predator to understand food web shifts through time because of their primarily piscivorous diet, generalist foraging strategies, high site fidelity, and frequent occurrence in museum specimen collections. Adult harbor seals typically forage 5–10 km from haul out sites and at depths <200 m (Lowry et al., 2001) and are opportunistic feeders (Lance et al., 2012). Therefore, the nitrogen and carbon stable isotope compositions of harbor seals offer a robust representation of the isotopic composition of carbon and nitrogen assimilated into coastal food webs. Harbor seal-specific trophic enrichment factors for nitrogen have been quantified in controlled feeding studies, confirming minimal trophic enrichment for phenylalanine between seals and their prey (Germain et al., 2013). Environmentally induced shifts in foraging patterns, specifically nearshore versus offshore feeding, has the potential to affect the carbon isotope composition in harbor seal tissues (Figure 1). We assume these behavioral effects are minimal on annual time scales compared to changes in the carbon

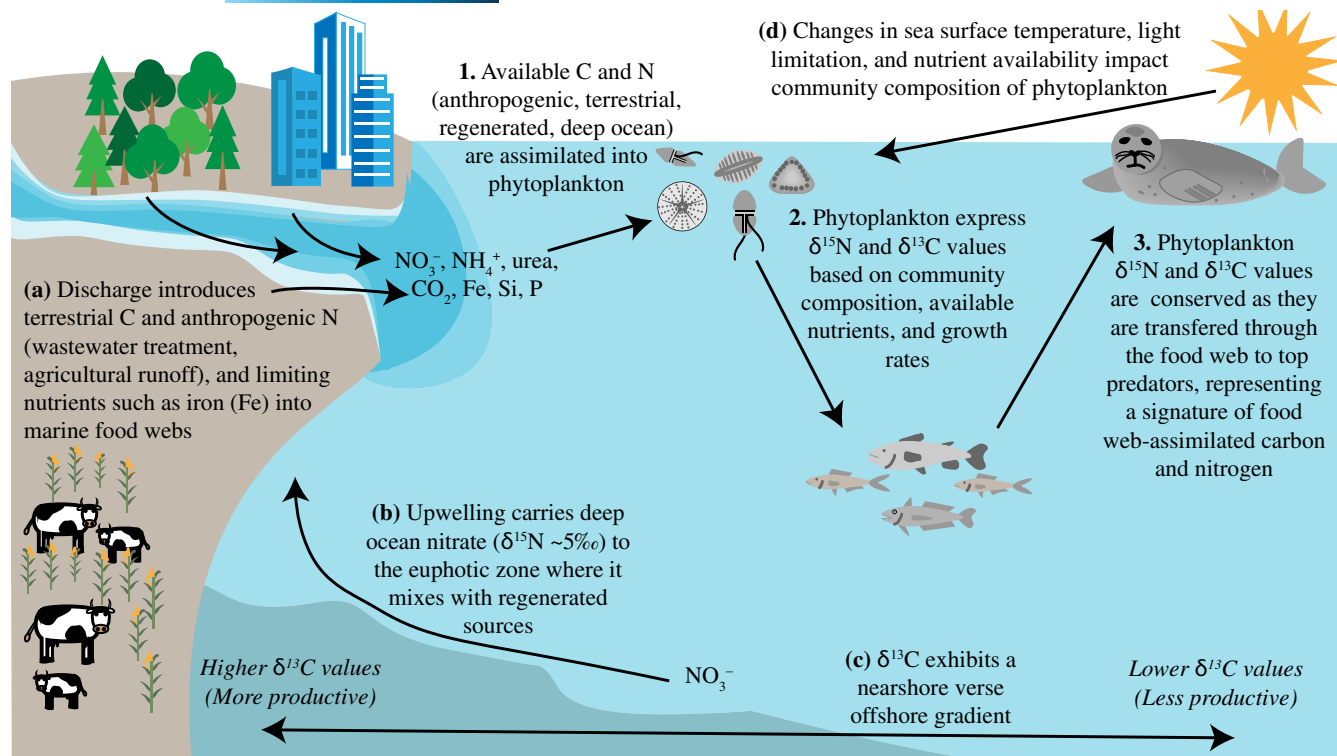


**FIGURE 1** Mechanisms of environmentally induced changes in nitrogen and carbon resources (a–d) which are assimilated into the stable isotope ratios of primary producers (1 and 2), and the stable isotope ratios of bulk  $\delta^{13}\text{C}$  and  $\delta^{15}\text{N}$  of phenylalanine are conserved when assimilated into consumers at higher trophic levels in the food web (3)

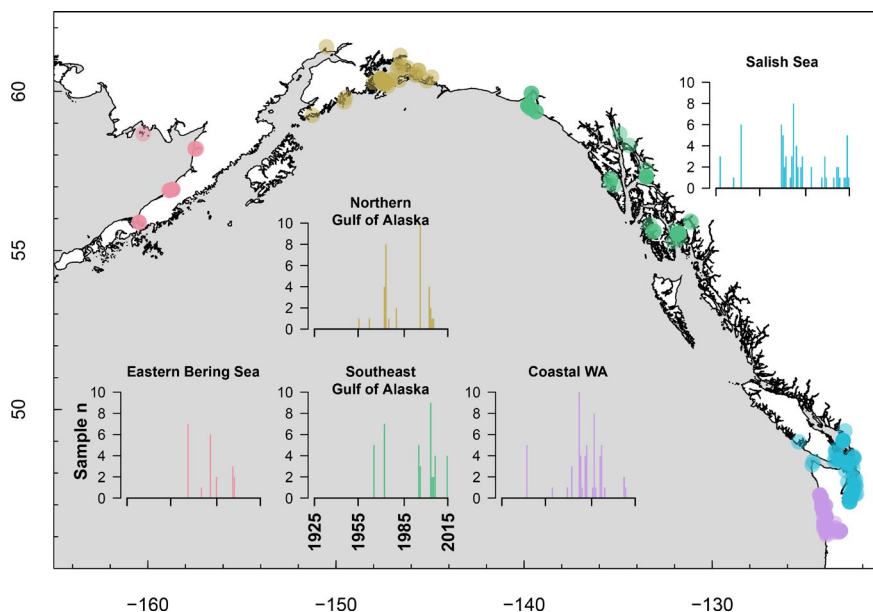


**FIGURE 2** Spatial and temporal distributions of northeast Pacific harbor seal specimens by subregion analyzed for  $\delta^{15}\text{N}_{\text{Phe}}$  and bulk  $\delta^{13}\text{C}$  values. Subplot colors correspond to map locations and x-axis (years) is the same for each subplot

and nitrogen isotope compositions at the base of the food web given their restricted foraging ranges.

We aim to identify how archived  $\delta^{15}\text{N}_{\text{Phe}}$  and bulk  $\delta^{13}\text{C}$  values vary regionally across the northeast Pacific on ecologically relevant scales (integrated annually and regionally) and through time using museum harbor seal specimens from 1928 to 2014 (Figure 2). Additionally, we characterize abiotic factors that influence harbor

seal  $\delta^{15}\text{N}_{\text{Phe}}$  and bulk  $\delta^{13}\text{C}$  values to identify ocean conditions important for food web assimilation of nitrogen and carbon. The effect of regional ocean condition on the stable isotope signature of source amino acids limits the application of short-term datasets for productivity studies, as short-term environmental perturbations are difficult to decouple from longer term trends such as climate regimes (Vokhshoori & McCarthy, 2014). We therefore identify long-term

environmental drivers that are important for interpreting reconstructed isotope data.

## 2 | MATERIALS AND METHODS

### 2.1 | Sample collection and analysis

Harbor seal bone samples were obtained from specimens curated at the Burke Museum (University of Washington), the Slater Museum (University of Puget Sound), the Museum of the North (University of Alaska Fairbanks), the Royal British Columbia Museum, the Smithsonian Institute, and the National Marine Mammal Laboratory (NOAA; Supporting Information S2, Table S1). Specimens were either treated by maceration in warm water or cleaned by beetles and soaked in a dilute ammonia solution then stored in acid free boxes. Adult specimens were sampled from three regions: eastern Bering Sea, the Gulf of Alaska, and Washington state, which also included 18 specimens from the southern British Columbia coast (Figure 2). We further stratified samples from the Gulf of Alaska into two subregions (northern and southeast) and Washington state into two subregions (coastal and Salish Sea) for a total of five subregions. Sampling prioritized long-term temporal coverage, specifically focusing on climate regimes shifts (i.e., Pacific Decadal Oscillation [PDO]). Additionally, samples with sex and size metadata were prioritized, although this information was not available for most specimens. Metadata were accessed through VertNet using catalogue numbers and institution codes (<http://www.vertnet.org/index.html>).

Bone samples were decalcified with the resulting collagen acid hydrolyzed, derivatized, and analyzed for compound-specific nitrogen stable isotope analysis (CSSIA) of 11 individual amino acids, including one source amino acid, phenylalanine (phe). Of the 11 amino acids, phenylalanine was the only discernable source amino acid and phenylalanine is the only amino acid data reported in this manuscript (Appendix S1). CSSIA samples were analyzed by GC-C-irMS at the University of Washington Facility for Compound-Specific Stable Isotope Analysis of Environmental Samples using a Thermo Scientific Trace GC + GC IsoLink coupled to a Delta V irMS following the procedures developed by Chikaraishi et al. (2007) and protocols by Rachel Jeffrey's laboratory at the University of Liverpool, UK (full analytical details are provided in Appendix S1). Individual collagen samples were analyzed in triplicate along with a mixed amino acid standard of known isotopic composition (Sigma-Aldrich Co.; mean precision of analytical standard for phenylalanine = 0.3‰). Internal and external standards were used and data processing included a drift correction. A total of 215 specimens were sampled from the time period of 1928–2014 for CSSIA, making this the largest CSSIA dataset of a mammal to date. Decalcified collagen of 190 specimens was analyzed for bulk  $^{13}\text{C}/^{12}\text{C}$  and bulk  $^{15}\text{N}/^{14}\text{N}$  at the University of Washington's IsoLab using a Costech ElementalAnalyzer, ConFlo III, MAT253 for continuous flow-based measurements.  $^{15}\text{N}/^{14}\text{N}$  and  $^{13}\text{C}/^{12}\text{C}$  are reported in standard delta notation:

$$\delta^{15}\text{N}(\text{‰ vs. air}) = \left( \frac{(^{15}\text{N}/^{14}\text{N})_{\text{Sample}}}{(^{15}\text{N}/^{14}\text{N})_{\text{Air}}} - 1 \right) * 1000, \quad (1)$$

$$\delta^{13}\text{C}(\text{‰ vs. VPBD}) = \left( \frac{(^{13}\text{C}/^{12}\text{C})_{\text{Sample}}}{(^{13}\text{C}/^{12}\text{C})_{\text{VPBD}}} - 1 \right) * 1000, \quad (2)$$

Internal laboratory standards (Bristol Bay salmon and glutamic acid) were interspersed with samples for a two-point calibration and blank correction (mean standard precision 0.09‰ for  $\delta^{15}\text{N}$  and 0.04‰ for  $\delta^{13}\text{C}$ ). A linear drift correction was also applied using IsoDat software. The collagen C:N ratio was used to verify the integrity of collagen for stable isotope analysis following specimen treatment and storage (van Klinken, 1999).

The isotopic composition of marine dissolved organic carbon has been steadily depleted in  $^{13}\text{C}$  over the past 100 years due to increases in anthropogenic  $\text{CO}_2$  in the atmosphere (referred to as the oceanic Suess effect; Quay et al., 1992).  $\delta^{13}\text{C}$  data were therefore corrected for the Suess effect using the following equation (Misarti et al., 2009):

$$\text{Suess effect correction factor} = d * e^{0.027 * (t - 1850)}, \quad (3)$$

where  $d$  is the maximum annual rate of  $\delta^{13}\text{C}$  decrease specific to the North Pacific (−0.014 derived from Quay et al., 1992) and  $t$  is the year represented by the year of specimen collection with a 1-year lag. The Suess effect varies regionally (Tagliabue & Bopp, 2008) and we applied a northeast Pacific parameterization (Misarti et al., 2009).

Standard linear models were used to identify whether size (standard length, cm), sex, and subregion of the harbor seals sampled were related to isotopic composition and to test whether these parameters needed to be standardized in environmental models.  $\delta^{15}\text{N}_{\text{phe}}$  and  $\delta^{13}\text{C}$  values were modeled independently as univariate continuous response variables using the following equation:

$$y_i \sim N(\alpha + \beta \mathbf{X}_i, \sigma_y^2), \quad (4)$$

where  $y$  is the mean triplicate value for each individual  $i$  for either  $\delta^{15}\text{N}_{\text{phe}}$  or  $\delta^{13}\text{C}$  values.  $\mathbf{X}$  represents the matrix of predictors (sex, length, subregion),  $\alpha$  is a scalar and  $\beta$  is a vector of coefficients for the predictors. Length ( $n = 116$ ) was modeled as a continuous variable and was natural log transformed; subregion and sex ( $n = 190$ ) were modeled as factors. Individual models were used to test whether a predictor was significant as opposed to a multivariate framework because, (1) sample sizes for  $\delta^{15}\text{N}_{\text{phe}}$  ( $n = 215$ ) and  $\delta^{13}\text{C}$  ( $n = 190$ ) data varied, and (2) predictor metadata were incomplete for specimens. A pairwise  $t$ -test using the Bonferroni correction and non-pooled standard deviation was also used to compare differences in mean isotope signature between subregions and sex (Figure 3; Tables S3 and S4).

To understand the extent of coupling between indices of food web-assimilated production and nitrogen resources, a linear model representing the basin wide relationship was fit to  $\delta^{13}\text{C}$  and  $\delta^{15}\text{N}_{\text{phe}}$  values as continuous variables assuming normal errors. To

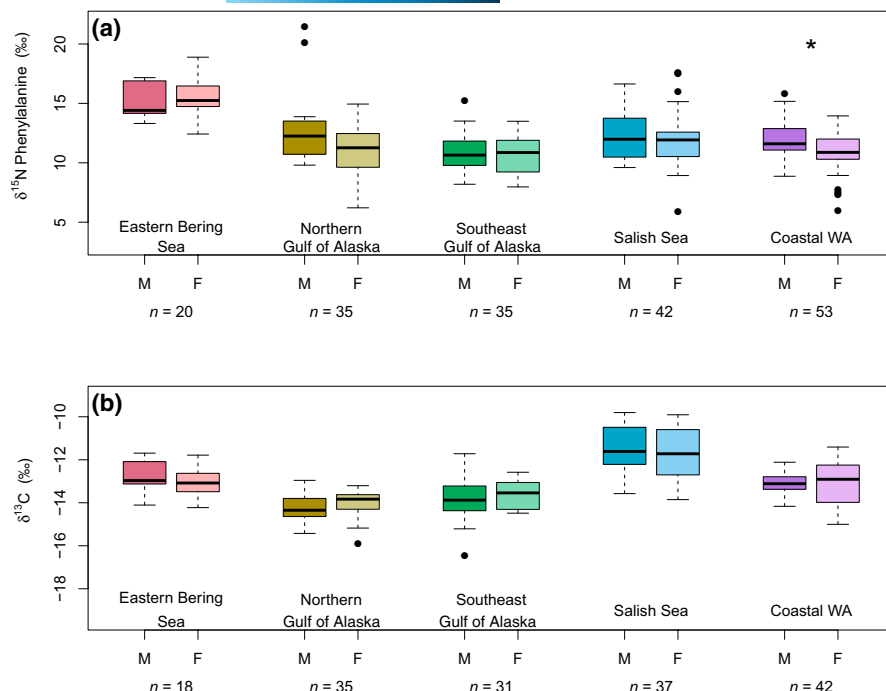


**FIGURE 3** Variability in  $\delta^{15}\text{N}_{\text{Phe}}$  and  $\delta^{13}\text{C}$  values based on subregion and sex. \*denotes a significant difference in isotopic signature between males and females for that region (colors correspond to Figure 2)

understand the spatial variation in this relationship, a hierarchical model was fit to the same dataset with varying slope and varying intercept based on subregion as a random effect. This model took the following form:

$$y_i \sim N(\alpha_{[j]} + \beta_{[j]}x_i, \sigma_y^2), \quad (5)$$

where  $y$  represents  $\delta^{13}\text{C}$  values as a continuous variable,  $x$  represents  $\delta^{15}\text{N}_{\text{Phe}}$  values as a continuous variable, and  $j$  represents the group level predictor, subregion.  $\alpha$  and  $\beta$  are each vectors of coefficients that vary by subregion.

## 2.2 | Quantifying effects of ocean condition on food web isotope indices

Linear models were used to identify environmental drivers of  $\delta^{13}\text{C}$  and  $\delta^{15}\text{N}_{\text{Phe}}$  values using a suite of environmental indices as covariates. A total of 42 environmental time series were compiled as potential predictor variables (Table S1) based on previous evidence for food web importance in the northeast Pacific (*sensu* Di Lorenzo et al., 2008; Stachura et al., 2014). Each environmental time series was standardized around a mean of 0 and standard deviation of 1 and discharge data were also natural log transformed. We divided these environmental covariates a priori into four main mechanistic properties based on the expected effect on nutrient assimilation into the food web: climate regime, freshwater discharge, circulation (wind and upwelling), and SST (Figure 1). Given the three regions in our analysis, each of these hypotheses was also divided according to our regional geographic breaks (eastern Bering Sea, Gulf of Alaska, and Washington). To reduce collinearity between environmental time series and reduce the total number of candidate models,

a subset of seven environmental time series were selected for each region based on the temporal overlap with stable isotope data. Each subset contained at least one time series for each of the four mechanistic properties (Table S2). While reduction in the number of time series provides analytical benefits, it comes at the cost of potentially conservative estimates of which covariates are important, meaning important components of ocean condition to the food webs may be missed.

$\delta^{15}\text{N}_{\text{Phe}}$  and  $\delta^{13}\text{C}$  values were independently considered as response variables to evaluate relationships between predictors (environmental indices and location) and stable isotope data using Equation (4) where  $X$  is a matrix of predictors using the seven standardized environmental time series (continuous) and subregion (factor) as covariates. We treated carbon and nitrogen isotopes as response variables separately in linear models, rather than in a combined multivariate model due to differences in sample size and differences in the strength of correlation between  $\delta^{15}\text{N}_{\text{Phe}}$  and  $\delta^{13}\text{C}$  values for each subregion. Time series data prior to 1950 and after 2014 were excluded from this analysis as data for some covariates did not extend beyond 1950. Candidate models ( $n = 53$ ) were compared using Akaike information criteria with a small sample size correction ( $\text{AIC}_c$ ; Akaike, 1973) and included all combinations of the environmental indices. In addition, a subregion factor was included with two levels for Washington (Salish Sea and coastal Washington) and the Gulf of Alaska (southcentral and southeast) and a null model (intercept only) was also tested. Tissue turnover time of bone collagen has not been measured in mammals of this size, to our knowledge, but is approximately 173 days for birds (Hobson & Clark, 1992). Thus, a lag of 1 year was applied to the stable isotope datasets to account for the timing of tissue turnover in bone collagen (additional lags were also considered, see Appendix S2). For each model with relatively high support ( $\Delta\text{AIC}_c < 2$ ), the  $\text{AIC}_c$  weight and the coefficient for

each covariate are reported (Figure 3). To confirm collinearity was not problematic in the candidate models that included more than one environmental covariate, matrix scatterplots and variance inflation factors (vif) were used from the car package (Fox & Weisberg, 2019) in R (R Core Team, 2019).

### 2.3 | Gaussian process dynamic factor analysis

To further understand how the environment,  $\delta^{13}\text{C}$ , and  $\delta^{15}\text{N}_{\text{Phe}}$  values covary through time in the Northeast Pacific, we developed a novel extension of conventional dynamic factor analysis (DFA). DFA is a dimension reduction technique that identifies common processes underlying a set of multivariate time series. This technique has been applied to multivariate time series problems in fisheries and ecology to identify patterns of oceanographic variability that drive Pacific salmon stocks (Jorgenson et al., 2016; Ohlberger et al. 2016; Stachura et al., 2014).

Dynamic factor analysis models identify common trends across multiple time series ("latent trends") and estimates the importance of that trend for each individual time series as a coefficient ("factor loading"). The two equations describing DFA take on the following form:

$$\mathbf{y}_t = \mathbf{Z}\mathbf{x}_t + \mathbf{v}_t, \text{ where } \mathbf{v}_t \sim \text{MVN}(\mathbf{0}, \mathbf{R}), \quad (6)$$

$$\mathbf{x}_t = \mathbf{x}_{t-1} + \mathbf{w}_t, \text{ where } \mathbf{w}_t \sim \text{MVN}(\mathbf{0}, \mathbf{I}). \quad (7)$$

The observed data  $\mathbf{y}_t$  are modeled as combinations of latent trends  $\mathbf{x}_t$  at time  $t$  (the dimensions of  $\mathbf{x}_t$  matching the number of trends which are also referred to as states) and factor loadings ( $\mathbf{Z}$ ; a coefficient for each time series for each trend) at time  $t$ , which are modeled as a random walk (Zuur et al., 2003). In addition there is an optional random observation error ( $\mathbf{v}_t$ ) and process error ( $\mathbf{w}_t$ ) which are multivariate normal.

Our extension of DFA adopts an alternative model of the latent trends, modeling them with Gaussian processes rather than random walks (Appendix S3). With conventional DFA using an autoregressive model, long gaps in time series data result in large overestimations of the variance of the latent trends. Gaussian processes model time series as a multivariate normal distribution, with estimated mean vector  $\mathbf{u}$  and covariance matrix  $\mathbf{\Sigma}$  (Munch et al. 2018). To constrain the number of estimated parameters, elements of  $\mathbf{\Sigma}$  were modeled with a Gaussian or squared covariance exponential function such that  $\Sigma_{ij} = \sigma^2 \exp\left(-\left(t_i - t_j\right)^2 / \theta\right)$ . In this parameterization,  $\sigma^2$  controls the variability of the stochastic process,  $\theta$  controls the rate of decay in correlation between time steps, and  $t_i$  and  $t_j$  are the time variables (e.g., years) for locations  $i$  and  $j$ .

We considered models with one to four underlying trends. Each trend was modeled separately (different means) but models with multiple trends have a shared covariance matrix among trends. The Gaussian process DFA (GPDFA) approach was applied to time series from each region and the best model was selected using

**TABLE 1** Range of  $\delta^{15}\text{N}_{\text{Phe}}$  and  $\delta^{13}\text{C}$  values observed in harbor seals for each of the five northeast Pacific subregions.

	$\delta^{15}\text{N}_{\text{Phe}}$ (‰)	$\delta^{13}\text{C}$ (‰)
Coastal WA	6.0–15.8	–15.6 to –11.8
Salish Sea	5.9–18.2	–16.6 to –6.8
Northern Gulf of Alaska	6.2–21.5	–16.7 to –12.5
Southeast Gulf of Alaska	8.0–15.2	–17.3 to –12.1
Eastern Bering Sea	12.4–18.9	–15.0 to –12.1

leave-one-out cross-validation from the loo package in R (Vehtari et al., 2017). The choice of knots affects the degree of smoothness, with more knots creating more smooth functions. We tested several different numbers of knots and found results to be qualitatively similar. Similar to the previous analysis, time series data prior to 1948 for Washington state and prior to 1940 and after 2008 for the Gulf of Alaska were excluded from this analysis. We fit GPDFA to data from each region including all of the initial 42 identified environmental time series for that region (Table S1),  $\delta^{15}\text{N}_{\text{Phe}}$ , and  $\delta^{13}\text{C}$  values, with location as a factor. We implemented GPDFA using the Stan language (Carpenter et al., 2017; Stan Development Team, 2019), and R (version 3.6.2; R Core Team, 2019) via R package rstan (version 2.21.2; Stan Development Team, 2019). Code to implement GPDFA is available at <https://github.com/mfeddern/CSIA-AA/blob/master/SourceData/Src/Analysis/gpdfa.stan>.

### 3 | RESULTS

$\delta^{15}\text{N}_{\text{Phe}}$  and bulk  $\delta^{13}\text{C}$  values did not vary by sex ( $p > 0.05$ ; Figure 3) or size for the individuals sampled ( $p > 0.05$ ; Figure S2). Spatial variation in harbor seal  $\delta^{15}\text{N}_{\text{Phe}}$  and  $\delta^{13}\text{C}$  values was observed on sub-regional scales.  $\delta^{15}\text{N}_{\text{Phe}}$  values were similar for harbor seals in the northern Gulf of Alaska ( $11.9 \pm 2.9$ , mean  $\pm 1$  SD), southeast Gulf of Alaska ( $10.8 \pm 1.7$ ), and coastal Washington ( $11.3 \pm 1.9$ ). The eastern Bering Sea had significantly higher  $\delta^{15}\text{N}_{\text{Phe}}$  values compared to other subregions ( $15.2 \pm 1.8$ ) followed by the Salish Sea ( $12.2 \pm 2.3$ ), which had similar  $\delta^{15}\text{N}_{\text{Phe}}$  values compared to the northern Gulf of Alaska (Figure 3; Table S3).  $\delta^{13}\text{C}$  values varied by subregion ( $p < 0.05$ ) with the exception of the Gulf of Alaska, where the northern ( $-14.6 \pm 0.9$ ) and southeast ( $-14.4 \pm 1.1$ ) subregions were not significantly different, and the eastern Bering Sea ( $-13.4 \pm 0.9$ ) and coastal Washington ( $-13.6 \pm 0.9$ ) were not significantly different (Figure 3; Table S4). The variation between subregions appeared to follow a latitudinal gradient, where harbor seal mean  $\delta^{13}\text{C}$  values were most enriched in  $^{13}\text{C}$  in the Salish Sea ( $-12.2 \pm 1.5$ ), and became more depleted from coastal Washington and into the Gulf of Alaska (Table 1).

The relationship between harbor seal  $\delta^{15}\text{N}_{\text{Phe}}$  and  $\delta^{13}\text{C}$  values also varied on subregional scales. There was a positive linear association between harbor seal  $\delta^{15}\text{N}_{\text{Phe}}$  and  $\delta^{13}\text{C}$  values in the combined northeast Pacific basin and Bering Sea model with a slope of 0.12 (Figure 4a). For the hierarchical subregion model, the eastern Bering Sea and coastal Washington demonstrated a similar relationship,



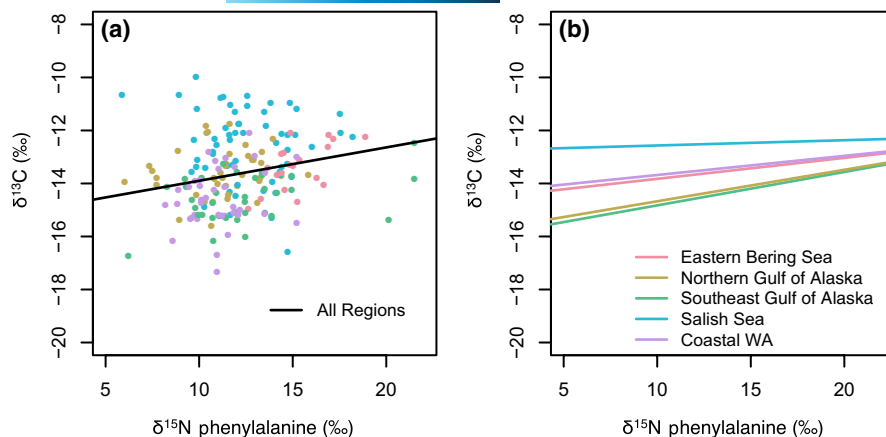


**FIGURE 4** Relationship between nitrogen sources ( $\delta^{15}\text{N}_{\text{Phe}}$ ) and primary production ( $\delta^{13}\text{C}$ ) assimilated into the food web for (a) a single linear model for the combined data across the northeast Pacific and eastern Bering Sea and (b) a mixed-effects model with random slope and intercept by subregion (colors correspond to Figure 2)

with slopes of 0.08 (95% CI [0.05, 0.11]) and 0.07 (95% CI [0.05, 0.09]), respectively. Similarly, harbor seals in both Gulf of Alaska subregions demonstrated comparable coupling of  $\delta^{15}\text{N}_{\text{Phe}}$  and  $\delta^{13}\text{C}$ , with slopes of 0.13 (95% CI [0.11, 0.14]) for the northern subregion and 0.12 (95% CI [0.10, 0.14]) for the southeastern subregion. Salish Sea harbor seals had a distinct relationship between  $\delta^{13}\text{C}$  and  $\delta^{15}\text{N}_{\text{Phe}}$  values relative to other subregions with a slope of only 0.02 that was not significantly different from 0 (95% CI [0.0, 0.04]; Figure 4b).

For both  $\delta^{15}\text{N}_{\text{Phe}}$  and  $\delta^{13}\text{C}$  values, there was substantial support for models including environmental indices rather than null or subregion-only models. The relationship between environmental indices and harbor seal  $\delta^{13}\text{C}$  and  $\delta^{15}\text{N}_{\text{Phe}}$  values in the northeast Pacific varied on regional scales. For Washington, the best model to predict harbor seal  $\delta^{15}\text{N}_{\text{Phe}}$  values included Columbia River discharge in high flow months, summer upwelling, and subregion. There was substantial model uncertainty for  $\delta^{15}\text{N}_{\text{Phe}}$  values in the Washington region; however, 90% of model weight supported the inclusion of Columbia River discharge (Figure 5a). The model for harbor seal  $\delta^{13}\text{C}$  values with the most support indicated a positive association between PDO, spring upwelling, and freshwater discharge in the Washington region (Figure 5b). In the Gulf of Alaska, the summer upwelling model had the most support as a predictor of harbor seal  $\delta^{15}\text{N}_{\text{Phe}}$  values with some model support for inclusion of the North Pacific Gyre Oscillation (NPGO), although the coefficients for this covariate did not differ substantially from 0 (Figure 5c). The best model for harbor seal  $\delta^{13}\text{C}$  values for the Gulf of Alaska included subregion, PDO, and NPGO (Figure 5d). In contrast to Washington, the Gulf of Alaska models supported a negative association between  $\delta^{13}\text{C}$  values and PDO. The null model for  $\delta^{15}\text{N}_{\text{Phe}}$  values in the eastern Bering Sea had the most support (Figure 5e). Lack of model support for environmental covariates in the eastern Bering Sea may have been a result of the small sample size in the region. Cross-shelf wind was included as a predictor in the best model (Figure 5f) for  $\delta^{13}\text{C}$  values in the eastern Bering Sea and was supported by 76% of the model weight.

Pacific Decadal Oscillation and Kuskokwim river discharge during high flow months were found to be highly collinear ( $\text{VIF} > 10$ ) and PDO was omitted from the candidate model set for the eastern Bering Sea analysis. All other models containing multiple environmental predictors with relative support had variance inflation factors less than 2 indicating only moderate collinearity across

covariates. Model residuals for the best models did not show trends through time (Figure S7). This indicates that there were no temporal trends associated with other ecosystem changes, such as harbor seal foraging strategy for example, after accounting for ocean condition. Model results did not change when using  $\delta^{13}\text{C}$  data that were not corrected for the regional Suess effect.

The GPDF analysis showed temporal synchronies and shared trends across environmental conditions and stable isotope values in the northeast Pacific. In the Gulf of Alaska, the data supported three latent trends (Figure 6). Both  $\delta^{15}\text{N}_{\text{Phe}}$  and  $\delta^{13}\text{C}$  values had the highest loadings for trend 1, which showed an increase starting in 1965 until 1980 followed by the trend oscillating at approximately 25% above the long-term average. The harbor seal  $\delta^{15}\text{N}_{\text{Phe}}$  values for the southeast subregion, harbor seal  $\delta^{13}\text{C}$  values, and spring upwelling had negative loadings on trend 1; loadings of  $\delta^{15}\text{N}_{\text{Phe}}$  values were generally weaker relative to loadings of  $\delta^{13}\text{C}$  values. For the other two trends (2 and 3), loadings were clustered by environmental driver category. Latent trend 2 oscillated around the long-term average and was uninformative. Trend 3 was below average starting in 1985 with strong loadings for climate time series, spring and summer upwelling, and discharge in high flow months (Figure 6). Annual discharge, autumn upwelling, Oceanic Niño Index, and Northern Oscillation Index did not demonstrate strong loadings for any trend. In Washington, there was support for two latent trends. Latent trend 1 shows a rapid increase in the 1940s to 25% above the long-term mean then a gradual decline until 1986 to approximately 40% below the long-term mean, with values below the mean starting in 1977 (Figure 7). Trend loadings for harbor seal  $\delta^{15}\text{N}_{\text{Phe}}$  and  $\delta^{13}\text{C}$  values were stronger for coastal seals and trend 1 had stronger loadings for freshwater discharge than trend 2. Trend 2 had strong loadings for  $\delta^{15}\text{N}_{\text{Phe}}$  and  $\delta^{13}\text{C}$  values for both Salish Sea and coastal Washington harbor seals. Trend 2 oscillated above and below the long-term mean and had large loadings for SST, summer upwelling, Fraser River discharge, and climate indices (Figure 7).

## 4 | DISCUSSION

We analyzed bone collagen  $\delta^{15}\text{N}_{\text{Phe}}$  and bulk  $\delta^{13}\text{C}$  values from harbor seal museum specimens collected between 1928 and 2014 as

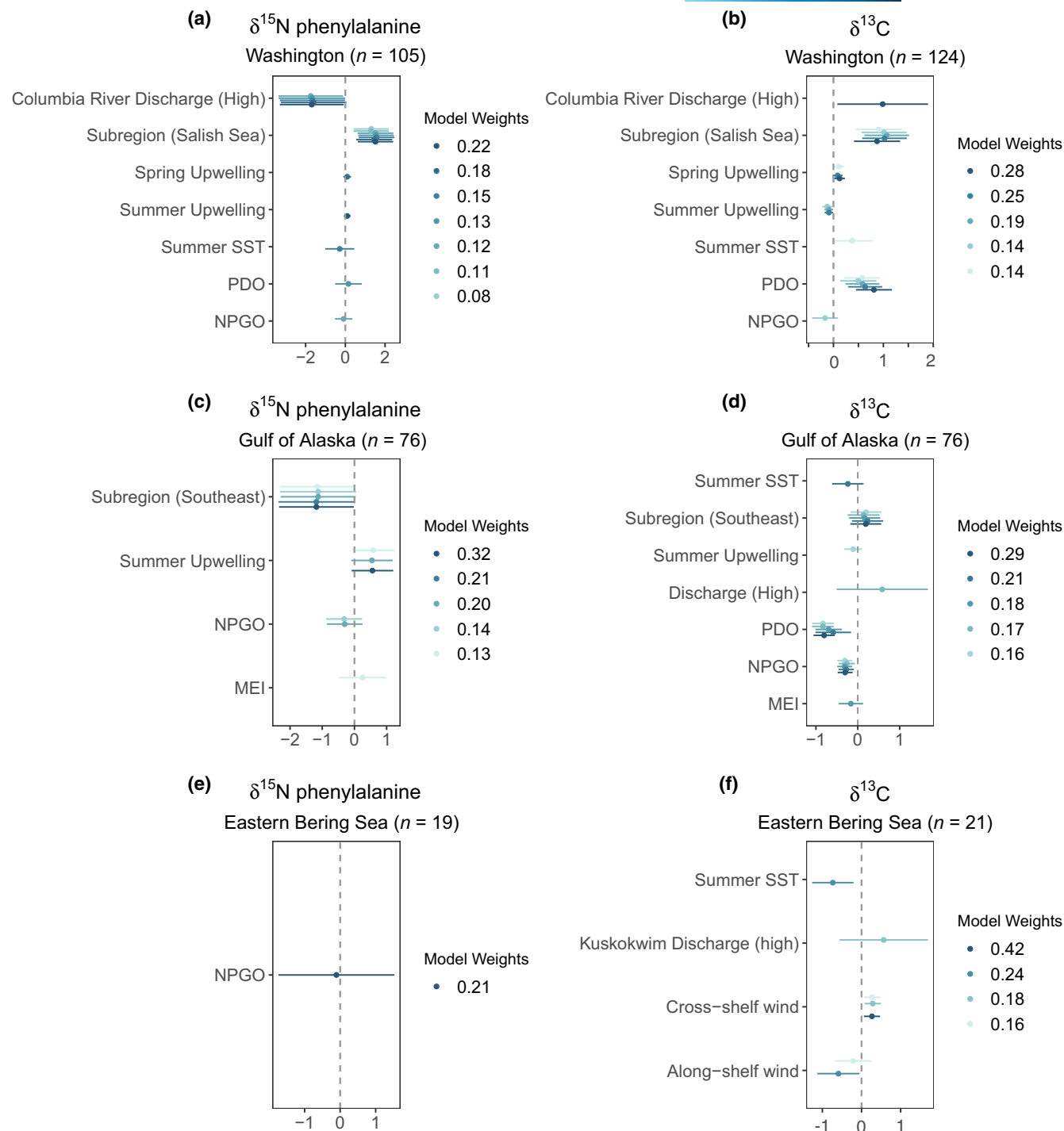


**FIGURE 5** Coefficients of environmental covariates for models with relative support ( $\Delta AIC_c < 2$ ) for harbor seal  $\delta^{15}N_{phe}$  and  $\delta^{13}C$  values in three regions of the northeast Pacific: Washington State, Gulf of Alaska, and the eastern Bering Sea. Color indicates model support based on AIC<sub>c</sub> weight; points are the coefficient estimates for each environmental covariate included in an individual model; bars show two standard deviations from the coefficient estimate

indices of change in food web assimilated nitrogen and carbon. Based on previous research (i.e., de la Vega et al. 2019, 2020; Graham et al., 2010; Lorrain et al. 2019; Sherwood et al., 2014), we interpret  $\delta^{15}N_{phe}$  and bulk  $\delta^{13}C$  values as primarily representing nitrogen and carbon resource utilization, and growth and community composition of primary producers at the base of the food web. Our data show the relationship between indices of primary production and nitrogen

resources assimilated into food webs varies regionally across the northeast Pacific. By pairing these data with environmental time series data, we provide new insights into large-scale environmental forcing that impacts the base of the food web and is transferred to higher trophic levels. Specifically, oceanic conditions associated with climate regimes and upwelling explain significant temporal variation in  $\delta^{15}N_{phe}$  and bulk  $\delta^{13}C$  values of coastal predators in northeast



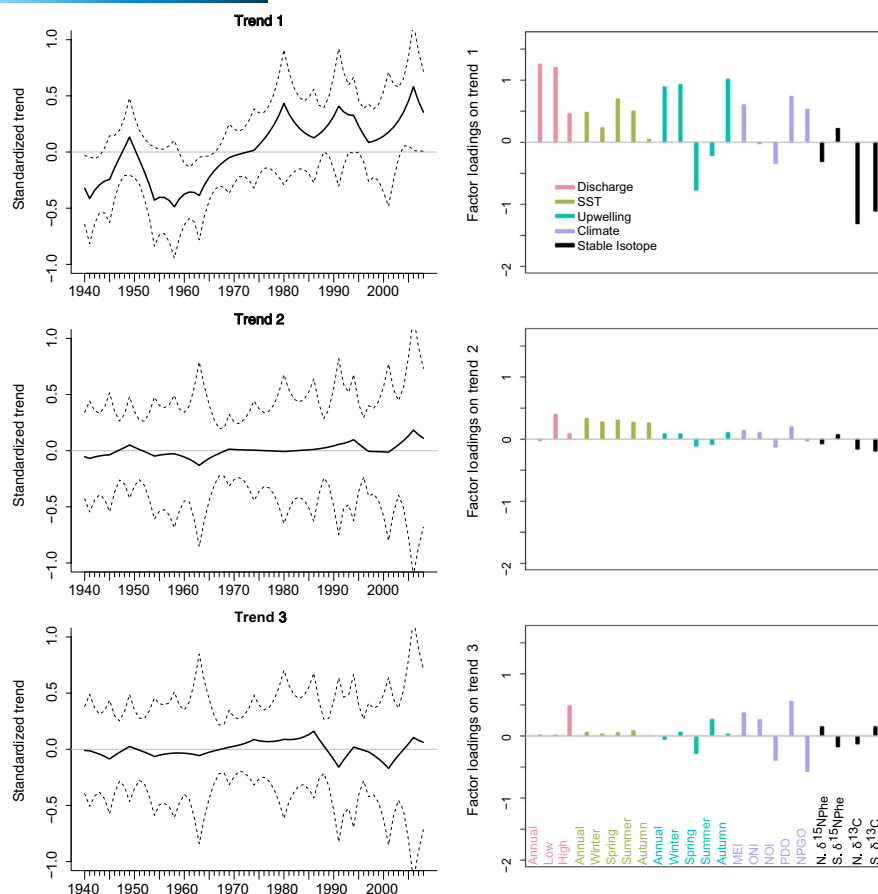


**FIGURE 6** Common trends in environmental condition and food web-assimilated stable isotope values for the regional Gulf of Alaska Gaussian-dynamic factor analysis model. The solid lines represent the modeled trends, where 0 is the long-term average and 1 and -1 represent the maximum and minimum possible values, respectively; the dash line is the 90% credible interval. Factor loadings can be interpreted as coefficients, representing the strength of association between the modeled trend and each observed environmental time series (colors represent a priori driver category). Values close to 0 mean the observed time series did not correlate with the corresponding trend, while values close to 1 show the observed time series closely matched the modeled trend. Negative loadings indicate an inverse relationship between the observed time series and modeled trend. Stable isotope times series are modeled separately for the northern (N.  $\delta^{15}\text{N}_{\text{Phe}}$ ; N.  $\delta^{13}\text{C}$ ) and southeast (S.  $\delta^{15}\text{N}_{\text{Phe}}$ ; S.  $\delta^{13}\text{C}$ ) subregions. Environmental times series are described in Table S1

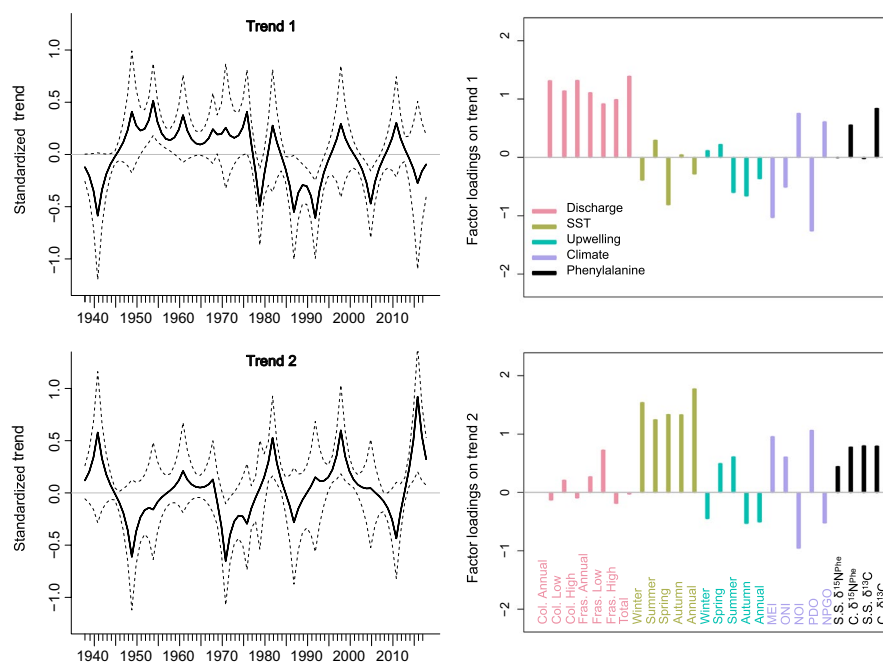


**FIGURE 7** Common trends in environmental condition and food web-assimilated stable isotope values for the regional Washington Gaussian-dynamic factor analysis model. Stable isotope times series are modeled separately for the coastal (C.  $\delta^{15}\text{N}_{\text{Phe}}$ ; C.  $\delta^{13}\text{C}$ ) and Salish Sea (S.S.  $\delta^{15}\text{N}_{\text{Phe}}$ ; S.S.  $\delta^{13}\text{C}$ ) subregions. See Figure 6 caption for further interpretation and Table S1 for descriptions of the environmental time series

Pacific (Figure 5; Figure S7). This analysis demonstrates that  $\delta^{15}\text{N}_{\text{Phe}}$  and bulk  $\delta^{13}\text{C}$  values are useful indicators of resources assimilated by coastal food webs.

#### 4.1 | Spatial variation in stable isotope indices

The geographically widespread association between harbor seal  $\delta^{15}\text{N}_{\text{Phe}}$  and  $\delta^{13}\text{C}$  values indicates that food web-assimilated primary production is coupled with nitrogen resources in most regions of the northeast Pacific, with the Salish Sea as a notable exception (Figure 4). Short-term studies in coastal Washington showed phytoplankton respond considerably to nitrogen inputs and are frequently nitrogen limited (Dortch & Postel, 1989; Kudela & Peterson, 2009). Similarly, short-term studies of the inner Gulf of Alaska shelf demonstrated primary production is generally nitrogen limited, and size, growth rates, and community composition are all tightly coupled with nutrient availability (Strom et al., 2006). A significant relationship between bulk  $\delta^{15}\text{N}$  and  $\delta^{13}\text{C}$  values was also observed in the tissues of some gorgonian corals over the same time period in coastal Gulf of Alaska (Williams et al., 2007). Given the evidence of nitrogen limitations and its relationship with phytoplankton growth and community composition in these coastal environments, the association between  $\delta^{15}\text{N}_{\text{Phe}}$  and  $\delta^{13}\text{C}$  values could be the result of nitrogen limiting growth at the base of the food web. Alternatively, the  $\delta^{15}\text{N}_{\text{Phe}}$  and  $\delta^{13}\text{C}$  coupling could be driven by covariance with an untested environmental variable that impacts most of the northeast Pacific but not the Salish Sea.

The coastal Washington and the Salish Sea food webs assimilate different nitrogen and carbon sources (Figure 5a,b). Salish Sea harbor seals have higher  $\delta^{15}\text{N}_{\text{Phe}}$  and  $\delta^{13}\text{C}$  values compared to individuals on the outer coast, which is likely due to significant contributions of intertidal producers and the legacy of anthropogenic N in the Salish Sea food web. Intertidal macrophytes (seagrass and algae) have similar  $\delta^{13}\text{C}$  values ( $\sim -10\text{‰}$ ) compared to harbor seals in the Salish Sea, while other potential sources are much lower (i.e., marine-derived sources  $\sim -20\text{‰}$ , terrestrial derived sources  $\sim -30\text{‰}$ ; Conway-Cranos et al., 2015; Howe & Simenstad, 2015). Incorporation of intertidal producers into the Salish Sea food web explains the difference in carbon stable isotope signatures between Salish Sea and coastal Washington harbor seals ( $\sim 1.4\text{‰}$ ; Figure 5a). However, it does not explain the higher  $\delta^{15}\text{N}_{\text{Phe}}$  values (Figure 5b; Table 1). Surface nitrate was observed to be  $8\text{‰} - 12\text{‰}$  off the coast of Washington in spring 1993 (Wu et al., 1997) which was exceeded by harbor seals in both coastal Washington and the Salish Sea (Table 1). It is likely anthropogenically derived nitrogen sources contribute to the higher observed  $\delta^{15}\text{N}_{\text{Phe}}$  values both directly and indirectly, particularly in the Salish Sea where harbor seal  $\delta^{15}\text{N}_{\text{Phe}}$  values were up to  $2.4\text{‰}$  higher than coastal Washington seals. Wastewater treatment facilities and agriculture runoff contribute substantial amounts ( $\sim 32\%$ ) of nitrogen in the Salish Sea (Mohamedali et al., 2011) and are enriched in  $^{15}\text{N}$ . In recent decades, Salish Sea waters have also been characterized by low dissolved oxygen and hypoxic events (PSEMP

Marine Waters Workgroup, 2019) from human-derived nitrogen loading. Anoxic conditions are conducive to denitrification, another potential indirect source of  $^{15}\text{N}$  from human activities in the region.

#### 4.2 | Ocean condition and stable isotope indices

Washington state food webs exhibit environmentally induced changes in assimilated primary production and nitrogen sources. The isotope–ocean condition relationship in the region can be explained by the introduction of terrestrial derived nutrients and climatically induced changes in phytoplankton community structure observed in previous studies (Du & Peterson, 2014; Du et al., 2015; Kudela et al., 2008). For example, the PDO has been associated with phytoplankton community shifts between dinoflagellates and diatoms in the northern California Current (Du et al., 2015). Similarly, the phytoplankton community composition is distinct in the early (spring) upwelling season compared to the late (summer) upwelling season (Du & Peterson, 2014). This could explain the inversely related associations between  $\delta^{13}\text{C}$  values and summer and spring upwelling (Figure 5b). Shifts in phytoplankton community structure are therefore a mechanism to explain the relationship between harbor seal  $\delta^{13}\text{C}$  values and ocean condition. In addition, freshwater discharge explains 16% of the variation observed in both  $\delta^{15}\text{N}_{\text{Phe}}$  and  $\delta^{13}\text{C}$  values in Washington. The Columbia River Plume introduces terrestrial derived nutrients, including nitrogen, and has been associated with increased primary production and fish production (Kudela et al., 2008; Ware & Thomson, 2005). The covariation between  $\delta^{15}\text{N}_{\text{Phe}}$ ,  $\delta^{13}\text{C}$ , and discharge indicates that isotopically distinct nitrogen resources introduced by freshwater discharge alter primary production, which is then assimilated into the Washington food web, and ultimately harbor seals.

In the eastern Bering Sea, our results suggest ice-born algae and  $^{15}\text{N}$  enriched nitrogen from the inner shelf are important for supporting the coastal food web. Recent evidence supports that consumer  $\delta^{15}\text{N}_{\text{Phe}}$  values reflect nitrate  $\delta^{15}\text{N}$  values in the arctic (de la Vega et al., 2020). However, our  $\delta^{15}\text{N}_{\text{Phe}}$  values from harbor seals of the eastern Bering Sea were high relative to previous studies of summer nitrate ( $5\text{‰} - 9\text{‰}$ ; Lehmann et al., 2005) and plankton nitrogen isotope signatures ( $6\text{‰} - 12\text{‰}$ ; Smith et al., 2002) from the outer and mid Bering Sea shelf. Morales et al. (2014) subsequently found the stable isotope composition of nitrogen in diatoms ranged from  $5\text{‰}$  to  $21\text{‰}$  in late winter and early spring. These values also increased in association with sea ice with a positive shoreward gradient (Morales et al. 2014). The range of sea-ice algae  $\delta^{15}\text{N}$  values observed by Morales et al. (2014) are consistent with our observed  $\delta^{15}\text{N}_{\text{Phe}}$  values in harbor seals (Table 1). Furthermore, the harbor seals in this study were located near the inner shelf in an area that has been partially covered by sea ice from January to May during the past century (Stabeno et al., 2007). Taken together, this indicates ice algae as a significant contributor to the coastal food web. The disconnect between the  $\delta^{15}\text{N}$  values of offshore nitrate (Lehmann et al. 2005) and harbor seals also highlights the problem in assuming

spatially and temporally discrete nitrate or phytoplankton measurements are representative of resources utilized by, and assimilated into, coastal food webs. Consumer  $\delta^{15}\text{N}_{\text{Phe}}$  measurements by their nature represent the N assimilated into the food web and integrated over relatively long time scales, while discrete measurements of nitrate may be spatially or temporally biased.

A short term (1998–2011) study of abiotic drivers in the Gulf of Alaska found chlorophyll-*a* anomalies were positive when downwelling favorable winds were low and had a negative relationship with sea level (Waite & Mueter, 2013). Similarly, Espinasse et al. (2020) found chlorophyll-*a*, SST, and sea level anomalies were the best predictors of carbon and nitrogen isotope data for secondary consumers over the past two decades. Our results agree with these studies as NPGO (an index of sea level) is negatively associated with both harbor seal  $\delta^{15}\text{N}_{\text{Phe}}$  (Figure 5c) and  $\delta^{13}\text{C}$  values (Figure 5d) in the Gulf of Alaska. Similarly, summer upwelling is positively associated with our  $\delta^{15}\text{N}_{\text{Phe}}$  values (Figure 5c). Based on our results, these environmentally induced changes represent long-term ecosystem dynamics that extend beyond merely the base of the food web and ultimately impact resources assimilated by top predators. In addition, regional climate indices characterize nutrient and primary production assimilated annually into the food web better than SST data alone. It is possible that other untested abiotic factors such as cross-shelf exchanges via eddy propagation or local wind stress (Waite & Mueter, 2013) may be important to food web-assimilated nitrogen and primary production in the Gulf of Alaska. Regardless, local variability in upwelling and basin scale indices of sea surface height and temperature (i.e., NPGO) ultimately determine resource assimilation in the Gulf of Alaska food web in which harbor seals forage.

By comparing consumer stable isotope values against environmental covariates across multiple subbasins, we show environmental forcing on coastal food webs is regionally distinct. For example, climate indices (i.e., PDO) in the Gulf of Alaska were inversely associated with food web-assimilated primary production (Figures 5d and 6 Trends 1 and 2) and positively associated in Washington (Figures 5b and 7 Trends 1 and 2). This agrees with previous studies where the PDO has been associated with alternating salmon production in the northeast Pacific (Mantua & Hare, 2002; Mantua et al., 1997). In cool phase years (i.e., 1947–1977), Washington stocks experience above average production and Alaska stocks experience below average production. Our results show that  $\delta^{13}\text{C}$  values for Washington and Gulf of Alaska also indicate alternating primary production between the two regions in association with PDO. Surprisingly,  $\delta^{13}\text{C}$  values are higher in cool phase years for the Gulf of Alaska (Figure 5d) and lower in cool phase years for Washington (Figure 5b). This suggests lower phytoplankton growth in Washington and higher phytoplankton growth in Gulf of Alaska in cool phase years. This is contrary to results of previous studies, assuming (1) higher  $\delta^{13}\text{C}$  values represent higher growth rates and (2) PDO is inhibiting growth at the base of the food web and indirectly constraining higher trophic levels such as salmon (Mantua & Hare, 2002; Mantua et al., 1997). It is likely the relationship between PDO, salmon production, and  $\delta^{13}\text{C}$  values of

harbor seals is instead caused by phytoplankton community structure influencing higher trophic levels rather than growth.

Common temporal trends in harbor seal stable isotopes and ocean condition empirically derived from the GPDF analysis (Figures 6 and 7) show changes in biogeochemical cycling and food web-assimilated production in recent decades that are associated with climatic variables. Since 1975, shared trends in environmental time series and stable isotope data in the Gulf of Alaska are above average for temperature, discharge, and NPGO and below average for assimilated  $\delta^{13}\text{C}$  values (as indicated by its negative loadings; Figure 6). Trends 2 and 3 in the Gulf of Alaska (Figure 6) show a distinct change in environmental indices starting in 1988. Loadings on these trends were higher for environmental indices than stable isotope data, suggesting a decoupling of environment–food web relationship in the region starting around 1988, which has also been observed between climate regimes and fish species (Litzow et al., 2020). This environment–food web decoupling was not observed in Washington (Figure 7) in our study or others (Litzow et al., 2020).

#### 4.3 | Using stable isotopes as food web indicators

Previous research has shown that lower trophic levels are sensitive to environmental variation in bottom-up drivers of productivity (*sensu* Frank et al., 2015; Jennings & Brander, 2010; Ware & Thompson, 2005), but few studies have demonstrated how the impact of these changes spans entire food webs on long time scales. By applying CSSIA to museum specimens of a generalist predator, we provide a novel piece of the ecological puzzle not previously available. First, these data provide a measure of changing nitrogen resources and phytoplankton dynamics that are spatially and temporally integrated for food web resource assimilation, rather than measuring the availability of inorganic nutrients or lower trophic level biomass and assuming an associated food web utilization. Dominant species of marine zooplankton exhibit selective foraging, particularly when resources are highly available (Bi & Sommer, 2020; Boersma et al. 2015; Jungbluth et al., 2017; Meunier et al., 2015), thus discrete measures of resources are not necessarily representative of what is utilized by the food web. Second, studies directly measuring primary production are often temporally limited to short time scales and recent decades. CSSIA of historic specimens allows for retrospective analyses that span long time scales (Mathews & Ferguson, 2014; McMahon et al., 2015, 2019; Sherwood et al., 2011) and thus identify long-term environmental forcing on food webs.

Despite these benefits, CSSIA (and stable isotope analysis data more generally) is limited in its ability to discern different mechanistic processes for isotopic enrichment in observational studies. Multiple mechanisms of fractionation often operate in tandem (Figure 1) and can be both additive and subtractive. For example, both the isotopic composition of dissolved inorganic nitrogen sources (primarily  $\text{NO}_3^-$ , but also urea and  $\text{NH}_4^+$ ) and the relative uptake of these sources impact the isotopic composition of nitrogen in primary producers (Graham et al., 2010; Ohkouchi et al., 2017). As a result, these data

on their own are limited in their ability to track exact mechanisms of fractionation and specific biogeochemical changes through time or space. Regardless, stable isotope signatures of nitrogen from source amino acids and bulk carbon can be used to trace variations in nitrogen sources at the base of the food web (i.e., de la Vega et al., 2020; Sherwood et al., 2014) and changes in phytoplankton dynamics (i.e., production, de la Vega et al., 2019; Lorrain et al., 2019) broadly. In addition, CSSIA of carbon is also emerging as a reliable proxy for phytoplankton community composition (Larsen et al., 2013; McMahon et al., 2015). We also assume a constant and small trophic enrichment factor for both bulk  $\delta^{13}\text{C}$  and  $\delta^{15}\text{N}_{\text{phe}}$  values. While trophic enrichment in  $\delta^{13}\text{C}$  and  $\delta^{15}\text{N}_{\text{phe}}$  values is minimal (Bocherens & Drucker, 2003; Germain et al., 2013; Hobson et al., 1996; Ohkouchi et al., 2017), and thus unlikely to impact overall correlations between datasets, it can produce enriched absolute isotope values and increased variation between observations (Nielsen et al., 2015), which was not accounted for in this study. Nonetheless, ours is among a number of supporting studies that show food webs are impacted by changing environmental conditions in the northeast Pacific (Cunningham et al. 2018; Puerta et al., 2019; Stachura et al., 2014).

Climate change will alter nutrient distributions and primary production throughout the world's oceans (Kwiatkowski et al., 2017; Marinov et al., 2010). Based on analysis of historical patterns of consumer isotopic variation with environmental forcing, we anticipate there will be region-specific spatial variability in how primary production and its dependent food webs respond to environmental change throughout the northeast Pacific over the next century. As environmental conditions (i.e., SST, discharge, anthropogenic nitrogen) continue to change, so will resources available to and assimilated by food webs. Given both resource availability and community composition of resources impact the function and stability of food webs (Narwani & Mazumder, 2012), it is likely that ecosystem interactions will change in response to environmentally induced shifts in resources. Understanding the dynamics influencing food web responses to their environment is important, as it provides information useful for predicting climate change impacts on aquatic resources and the communities and economies that depend on them.

## ACKNOWLEDGMENTS

We extend our deepest gratitude to our museum collaborators for permitting sampling and coordinating logistics. Specifically, we thank Jeff Bradley and Sharlene Santana of the UW Burke Museum, Peter Wimberger and Gary Shugart of the Slater Museum, Link Olson and Aren Gunderson of the Museum of the North, Robert DeLong of the National Marine Mammal Laboratory, Lesley Kennes and Gavin Hanke of the Royal BC Museum, and Darrin Lunde and John Osofsky of the Smithsonian Institute. We thank Megan Stachura and Tom Royer for assistance with environmental datasets, and Chris Harvey and Jens Nielsen for helpful discussions and support. Hyejoo Ro and Karrin Leazer assisted in laboratory work. Mark Haught and Terry Rolfe assisted with GC/C/IRMS method development, maintenance, and troubleshooting. This publication was funded in part by grants

from Washington Sea Grant, University of Washington, pursuant to National Oceanic and Atmospheric Administration award nos. NA18OAR4170095 and NA19OAR4170360. This publication is partially funded by the Joint Institute for the Study of the Atmosphere and Ocean (JISAO) under NOAA Cooperative Agreement NA15OAR4320063, contribution no. 2020-1116. Additional funding was provided by an internal grant from the Northwest Fisheries Science Center. The views expressed herein are those of the authors and do not necessarily reflect the views of NOAA or any of its sub-agencies.

## DATA AVAILABILITY STATEMENT

The data that supports the findings of this study are available in the Supporting Information of this article (Supporting Information S2) and <https://github.com/mfeddern/CSIA-AA/tree/master/SourceData>.

## ORCID

Megan L. Feddern  <https://orcid.org/0000-0002-5863-7229>

Gordon W. Holtgrieve  <https://orcid.org/0000-0002-4451-3567>

Eric J. Ward  <https://orcid.org/0000-0002-4359-0296>

## REFERENCES

- Akaike, H. (1973). Information theory and an extension of the maximum likelihood principle. In B. N. Petrov & F. Csäki (Eds.), *2nd International symposium on information theory* (pp. 199–213). Akademiai Kiadó.
- Bi, R., & Sommer, U. (2020). Food quantity and quality interactions at phytoplankton-zooplankton interface: Chemical and reproductive responses in a calanoid copepod. *Frontiers in Marine Science*, 7, 274.
- Bocherens, H., & Drucker, D. (2003). Trophic level isotopic enrichment of carbon and nitrogen in bone collagen: Case studies from recent and ancient terrestrial ecosystems. *International Journal of Osteoarchaeology*, 13, 46–53. <https://doi.org/10.1002/oa.662>
- Boersma, M., Mathew, K. A., Niehoff, B., Schoo, K. L., Franco-Santos, R. M., & Meunier, C. L. (2015). Temperature driven changes in the diet preference of omnivorous copepods: No more meat when it's hot? *Ecology Letters*, 19, 45–53. <https://doi.org/10.1111/ele.12541>
- Bonan, G. B., & Doney, S. C. (2018). Climate, ecosystems, and planetary futures: The challenge to predict life in Earth system models. *Science*, 359, eaam8328. <https://doi.org/10.1126/science.aam8328>
- Bopp, L., Resplandy, L., Orr, J. C., Doney, S. C., Dunne, J. P., Gehlen, M., Halloran, P., Heinze, C., Ilyina, T., Séférian, R., Tjiputra, J., & Vichi, M. (2013). Multiple stressors of ocean ecosystems in the 21st century: Projections with CMIP5 models. *Biogeosciences*, 10, 6225–6245. <https://doi.org/10.5194/bg-10-6225-2013>
- Brander, K. (2010). Impacts of climate change on fisheries. *Journal of Marine Systems*, 79, 389–402. <https://doi.org/10.1016/j.jmarsys.2008.12.015>
- Briatburg, D., Levin, L. A., Oschlies, A., Grégoire, M., Chavez, F. P., Conley, D. J., Garçon, V., Gilbert, D., Gutiérrez, D., Isensee, K., Jacinto, G. S., Limburg, K. E., Montes, I., Naqvi, S. W. A., Pitcher, G. C., Rabalais, N. N., Roman, M. R., Rose, K. A., Seibel, B. A., ... Zhang, J. (2018). Declining oxygen in the global ocean and coastal waters. *Science*, 359, eaam7240. <https://doi.org/10.1126/science.aam7240>
- Burkhardt, S., Riebesell, U., & Zondervan, I. (1999). Effects of growth rate,  $\text{CO}_2$  concentration, and cell size on the stable

- carbon isotope fractionation in marine phytoplankton. *Geochimica Et Cosmochimica Acta*, 63, 3729–3741. [https://doi.org/10.1016/S0016-7037\(99\)00217-3](https://doi.org/10.1016/S0016-7037(99)00217-3)
- Carpenter, B., Gelman, A., Hoffman, M. D., Lee, D., Goodrich, B., Betancourt, M., Brubaker, M. A., Guo, J., Li, P., & Riddell, A. (2017). Stan: A probabilistic programming language. *Journal of Statistical Software*, 76, 1–37. <https://doi.org/10.18637/jss.v076.i01>
- Chikaraishi, Y., Kashiyama, Y., Ogawa, N. O., Kitazato, H., & Ohkouchi, N. (2007). Metabolic control of nitrogen isotope composition of amino acids in macroalgae and gastropods: Implications for aquatic food web studies. *Marine Ecology Progress Series*, 342, 85–90. <https://doi.org/10.3354/meps342085>
- Chikaraishi, Y., Ogawa, N. O., Kashiyama, Y., Takano, Y., Suga, H., Tomitani, A., Miyashita, H., Kitazato, H., & Ohkouchi, N. (2009). Determination of aquatic food-web structure based on compound-specific nitrogen isotopic composition of amino acids. *Limnology and Oceanography Methods*, 7, 740–750. <https://doi.org/10.4319/lom.2009.7.740>
- Conway-Cranos, L., Kiffney, P., Banas, N., Plummer, M., Naman, S., MacCready, P., Bucci, J., & Ruckelshaus, M. (2015). Stable isotopes and oceanographic modeling reveal spatial and trophic connectivity among terrestrial, estuarine, and marine environments. *Marine Ecology Progress Series*, 533, 15–28. <https://doi.org/10.3354/meps11318>
- Cunningham, C. J., Westley, P. A. H., & Adkinson, M. D. (2018). Signals of large scale climate drivers, hatchery enhancement, and marine factors in Yukon River Chinook salmon survival revealed with a Bayesian life history model. *Global Change Biology*, 24, 4399–4416. <https://doi.org/10.1111/gcb.14315>
- de la Vega, C., Jeffreys, R. M., Tuerena, R., Ganeshram, R., & Mahaffey, C. (2019). Temporal and spatial trends in marine carbon isotopes in the Arctic Ocean and implications for food web studies. *Global Change Biology*, 25, 4116–4130. <https://doi.org/10.1111/gcb.14832>
- de la Vega, C., Mahaffey, C., Tuerena, R. E., Yurkowski, D. J., Ferguson, S. H., Stenson, G. B., Nordøy, E. S., Haug, T., Biuw, M., Smout, S., Hopkins, J., Tagliabue, A., & Jeffreys, R. M. (2020). Arctic seals as tracers of environmental and ecological change. *Limnology and Oceanography Letters*. <https://doi.org/10.1002/lol2.10176>
- Di Lorenzo, E., Schneider, N., Cobb, K. M., Chhak, K., Franks, P. J. S., Miller, A. J., McWilliams, J. C., Bograd, S. J., Arango, H., Curchister, E., Powell, T. M., & Rivere, P. (2008). North Pacific Gyre Oscillation links ocean climate and ecosystem change. *Geophysical Research Letters*, 35, L08607. <https://doi.org/10.1029/2007GL032838>
- Dortch, Q., & Postel, J. R. (1989). Biochemical indicators of N utilization by phytoplankton during upwelling off the Washington coast. *Limnology and Oceanography*, 34, 758–773. <https://doi.org/10.4319/lo.1989.34.4.0758>
- Du, X., & Peterson, W. T. (2014). Seasonal cycle of phytoplankton community composition in the coastal upwelling system off central Oregon in 2009. *Estuaries and Coasts*, 37, 299–311. <https://doi.org/10.1007/s12237-013-9679-z>
- Du, X., Peterson, W., & O'Higgins, L. (2015). Interannual variations in phytoplankton community structure in the northern California Current during the upwelling seasons of 2001–2010. *Marine Ecology Progress Series*, 519, 75–87. <https://doi.org/10.3354/meps11097>
- Espinasse, B., Hunt, B. P., Batten, S. D., & Pakhomov, E. A. (2020). Defining isoscapes in the Northeast Pacific as an index of ocean productivity. *Global Ecology and Biogeography*, 29, 246–261. <https://doi.org/10.1111/geb.13022>
- Fox, J., & Weisberg, S. (2019). *An R companion to applied regression* (3rd ed.). Sage.
- Frank, K. T., Fisher, J. A. D., & Leggett, W. C. (2015). The spatio-temporal dynamics of trophic control in large marine ecosystems. In T. C. Hanley & K. J. La Pierre (Eds.), *Trophic ecology* (pp. 31–54). Cambridge University Press.
- Fry, B. (2006). Using stable isotope tracers. In *Stable isotope ecology* (pp. 40–75). Springer.
- Germain, L. R., Koch, P. L., Harvey, J., & McCarthy, M. D. (2013). Nitrogen isotope fractionation in amino acids from harbor seals: Implications for compound-specific trophic position calculations. *Marine Ecology Progress Series*, 482, 265–277. <https://doi.org/10.3354/meps10257>
- Graham, B. S., Koch, P. L., Newsome, S. D., McMahon, K. W., & Aurioles, D. (2010). Using isoscapes to trace the movements and foraging behavior of top predators in the oceanic ecosystem. In J. B. West, G. J. Bowen, T. E. Dawson, & K. P. Tu (Eds.), *Isoscapes* (pp. 299–318). Spring.
- Gregg, W. W., Konkright, M. E., Ginoux, P., O'Reilly, J. E., & Casey, N. W. (2003). Ocean primary production and climate: Global decadal changes. *Geophysical Research Letters*, 30, 1809. <https://doi.org/10.1029/2003GL016889>
- Hobson, K. A., & Clark, R. G. (1992). Assessing avian diets using stable isotopes I: Turnover of  $^{13}\text{C}$  in tissues. *The Condor*, 94, 181–188. <https://doi.org/10.2307/1368807>
- Hobson, K. A., Schell, D. M., Renouf, D., & Noseworthy, E. (1996). Stable carbon and nitrogen isotopic fractionation between diet and tissues of captive seals: Implications for dietary reconstruction involving marine mammals. *Canadian Journal of Fisheries and Aquatic Sciences*, 53, 528–533. <https://doi.org/10.1139/z00-008>
- Hoegh-Guldberg, O., & Bruno, J. F. (2010). The impact of climate change on the world's marine ecosystems. *Science*, 328, 1523–1528. <https://doi.org/10.1126/science.1189930>
- Howe, E. R., & Simenstad, C. A. (2015). Using stable isotopes to discern mechanisms of connectivity in estuarine detritus-based food webs. *Marine Ecology Progress Series*, 518, 13–29. <https://doi.org/10.1139/z00-008>
- Jennings, S., & Brander, K. (2010). Predicting the effects of climate change on marine communities and the consequences for fisheries. *Journal of Marine Systems*, 79, 418–426. <https://doi.org/10.1016/j.jmarsys.2008.12.016>
- Jorgenson, J. C., Ward, E. J., Scheuerell, M. D., & Zabel, R. W. (2016). Assessing spatial covariance among time series of abundance. *Ecology and Evolution*, 6, 2472–2485. <https://doi.org/10.1002/ece3.2031>
- Jungbluth, M. J., Selph, K. E., Lenz, P. H., & Goetze, E. (2017). Species-specific grazing and significant trophic impacts by two species of copepod nauplii, *Parvocalanus crassirostris* and *Bestiolina similis*. *Marine Ecology Progress Series*, 572, 57–76. <https://doi.org/10.3354/meps12139>
- Kudela, R. M., Banas, N. S., Barth, J. A., Frame, E. R., Jay, D. A., Largier, J. L., Lessard, E. J., Peterson, T. D., & Vander Woude, A. J. (2008). Controls and mechanisms of plankton productivity in coastal upwelling waters of the northern California Current system. *Oceanography*, 46, 46–59.
- Kudela, R., & Peterson, T. D. (2009). Influence of a buoyant river plume on phytoplankton nutrient dynamics: What controls standing stocks and productivity? *Journal of Geophysical Research*, 114, C00B11. <https://doi.org/10.1029/2008JC004913>
- Kwiatkowski, L., Bopp, L., Aumont, O., Ciais, P., Cox, P. M., Laufkötter, C., Li, Y., & Séférian, R. (2017). Emergent constraints on projections of declining primary production in the tropical oceans. *Nature Climate Change*, 7, 355–358. <https://doi.org/10.1038/nclimate3265>
- Lance, M. M., Wan-Ying, C., Jeffries, S. J., Pearson, S. F., & Acevedo-Gutiérrez, A. (2012). Harbor seal diet in northern Puget Sound: implications for the recovery of depressed fish stocks. *Marine Ecology Progress Series*, 464, 257–271. <https://doi.org/10.3354/meps09880>
- Larsen, T., Ventura, M., Andersen, N., O'Brien, D. M., Piatkowski, U., & McCarthy, M. D. (2013). Tracing carbon sources through aquatic and terrestrial food webs using amino acid stable isotope fingerprinting. *PLoS One*, 8(9), e73441. <https://doi.org/10.1371/journal.pone.0073441>



- Lehmann, M. F., Sigman, D. M., McCorkle, D. C., Brunelle, B. G., Hoffmann, S., Kienast, M., Cane, G., & Clement, J. (2005). Origin of the deep Bering Sea nitrate deficit: Constraints from the nitrogen and oxygen isotopic composition of water column nitrate and benthic nitrate fluxes. *Global Biogeochemical Cycles*, 19, GB4005. <https://doi.org/10.1029/2005GB002508>
- Litzow, M. A., Hunsicker, M. E., Bond, N. A., Burke, B. J., Cunningham, C. J., Gosselin, J. L., Norton, E. L., Ward, E. J., & Zador, S. G. (2020). The changing physical and ecological meanings of North Pacific Ocean climate indices. *Proceedings of the National Academy of Sciences of the United States of America*, 117, 7665–7671. <https://doi.org/10.1073/pnas.1921266117>
- Lorrain, A., Pethybridge, H., Cassar, N., Receveur, A., Allain, V., Bodin, N., Bopp, L., Choy, C. A., Duffy, L., Fry, B., Goñi, N., Graham, B. S., Hobday, A. J., Logan, J. M., Ménard, F., Menkes, C. E., Olson, R. J., Pagendam, D. E., Point, D., ... Young, J. W. (2019). Trends in tuna carbon isotopes suggest global changes in pelagic phytoplankton communities. *Global Change Biology*, 26, 458–470. <https://doi.org/10.1111/gcb.14858>
- Lowry, L. F., Frost, K. J., Ver Hoep, J. M., & Delong, R. A. (2001). Movements of satellite-tagged subadult and adult harbor seals in Prince William Sound, Alaska. *Marine Mammal Science*, 17, 835–861. <https://doi.org/10.1111/j.1748-7692.2001.tb01301.x>
- Mantua, N. J., & Hare, S. R. (2002). The Pacific decadal oscillation. *Journal of Oceanography*, 58, 35–44.
- Mantua, N. J., Hare, S. R., Zhang, Y., Wallace, J. M., & Francis, R. C. (1997). A Pacific interdecadal climate oscillation with impacts on salmon production. *Bulletin of the American Meteorological Society*, 78, 1069–1079. [https://doi.org/10.1175/1520-0477\(1997\)078%3C1069:APICOW%3E2.0.CO;2](https://doi.org/10.1175/1520-0477(1997)078%3C1069:APICOW%3E2.0.CO;2)
- Marinov, I., Doney, S. C., & Lima, I. D. (2010). Response of ocean phytoplankton community structure to climate change over the 21st century: Partitioning the effects of nutrients, temperature and light. *Biogeosciences*, 7, 3941–3959. <https://doi.org/10.5194/bg-7-3941-2010>
- Mathews, C. J. D., & Ferguson, S. H. (2014). Spatial segregation and similar triophi-level diet among eastern Canadian Arctic/north-west Atlantic killer whales inferred from bulk and compound specific isotopic analysis. *Journal of the Marine Biological Association of the United Kingdom*, 94(6), 1343–1355.
- McCann, K. S., Rasmussen, U. J., & Umbanhowar, J. (2005). The dynamic of spatially coupled food webs. *Ecology Letters*, 8, 513–523. <https://doi.org/10.1111/j.1461-0248.2005.00742.x>
- McClelland, J. W., & Montoya, J. W. (2002). Trophic relationships and the nitrogen isotopic composition of amino acids in plankton. *Ecology*, 83, 2173–2180. [https://doi.org/10.1890/0012-9658\(2002\)083%5B2173:TRATNI%5D2.0.CO;2](https://doi.org/10.1890/0012-9658(2002)083%5B2173:TRATNI%5D2.0.CO;2)
- McMahon, K. W., McCarthy, M. D., Sherwood, O. A., Larsen, T., & Guilderson, T. P. (2015). Millennial-scale plankton regime shifts in the subtropical North Pacific Ocean. *Science*, 350, 1530–1533. <https://doi.org/10.1126/science.aaa9942>
- McMahon, K. W., Michelson, C. I., Hart, T., McCarthy, M. D., Patterson, W. P., & Polito, M. J. (2019). Divergent trophic responses of sympatric penguin species to historic anthropogenic exploitation and recent climate change. *Proceedings of the National Academy of Sciences of the United States of America*, 116, 25721–25727. <https://doi.org/10.1073/pnas.1913093116>
- Meunier, C. L., Boersma, M., Wiltshire, K. H., & Malzahn, A. M. (2015). Zooplankton eat what they need: Copepod selective feeding and potential consequences for marine systems. *Oikos*, 125, 50–58. <https://doi.org/10.1111/oik.02072>
- Misarti, N., Finney, B., Maschner, H., & Wooller, M. J. (2009). Changes in the northeast Pacific marine ecosystems over the last 4500 years: Evidence from stable isotope analysis of bone collagen from archaeological middens. *The Holocene*, 19, 1139–1151. <https://doi.org/10.1177/0959683609345075>
- Mohamedali, T., Roberts, M., Sackmann, B. S., & Kolosseus, A. (2011). *Puget Sound dissolved oxygen model: Nutrient load summary for 1999–2008*. Publication no. 11-03-057. Washington State Department of Ecology.
- Moore, J. K., Fu, W., Primeau, F., Britten, G. L., Lindsay, K., Long, M., Dney, S. C., Mahowald, N., Hoffman, F., & Randerson, J. T. (2018). Sustained climate warming drives declining marine biological productivity. *Science*, 359, 1139–1143. <https://doi.org/10.1126/science.aao6379>
- Morales, L. V., Granger, J., Chang, B. X., Prokopenko, M. G., Plessen, B., Gradinger, R., & Sigman, D. M. (2014). Elevated  $^{15}\text{N}/^{14}\text{N}$  in particulate organic matter, zooplankton, and diatom frustule-bound nitrogen in the ice-covered water column of the Bering Sea eastern shelf. *Deep Sea Research Part II: Topical Studies in Oceanography*, 109, 100–111. <https://doi.org/10.1016/j.dsr2.2014.05.008>
- Munch, S. B., Giron-Nava, A., & Sugihara, G. (2018). Nonlinear dynamics and noise in fisheries recruitment: A global meta-analysis. *Fish and Fisheries*, 19, 964–973. <https://doi.org/10.1111/faf.12304>
- Narwani, A., & Mazumder, A. (2012). Bottom-up effects of species diversity on the functioning and stability of food webs. *Journal of Animal Ecology*, 81, 701–713. <https://doi.org/10.1111/j.1365-2656.2011.01949.x>
- Nielsen, J. M., Popp, B. N., & Winder, M. (2015). Meta-analysis of amino acid stable nitrogen isotope ratios for estimating trophic position in marine organisms. *Oecologia*, 178, 631–642. <https://doi.org/10.1007/s00442-015-3305-7>
- Ohkouchi, N., Chikaraishi, Y., Close, H. G., Fry, B., Larsen, T., Madigan, D. J., McCarthy, M. D., McMahon, K. W., Nagata, T., Naito, Y. I., Ogawa, N. O., Popp, B. N., Steffan, S., Takano, Y., Tayasu, I., Wyatt, A. S. J., Yamaguchi, Y. T., & Yokoyama, Y. (2017). Advances in the application of amino acid nitrogen isotopic analysis in ecological and biogeochemical studies. *Organic Geochemistry*, 113, 150–174. <https://doi.org/10.1016/j.orggeochem.2017.07.009>
- Ohlberger, J., Scheuerell, M. D., & Schindler, D. E. (2016). Population coherence and environmental impacts across spatial scales: a case study of Chinook salmon. *Ecosphere*, 7, e01333. <https://doi.org/10.1002/ecs2.1333>
- PSEMP Marine Waters Workgroup. (2019). *Puget sound marine waters: 2018 overview*. S. K. Moore, R. Wold, B. Curry, K. Stark, J. Bos, P. Williams, N. Hamel, J. Apple, S. Kim, A. Brown, C. Krembs, & J. Newton (Eds.).
- Puerta, P., Ciannelli, L., Rykaczewski, R. R., Opiekun, M., & Litzow, M. A. (2019). Do Gulf of Alaska fish crustacean populations show synchronous non-stationary responses to climate? *Progress in Oceanography*, 175, 161–170. <https://doi.org/10.1016/j.pocean.2019.04.002>
- Quay, P. D., Tilbrook, B., & Wong, C. S. (1992). Oceanic uptake of fossil-fuel  $\text{CO}_2$ - $^{13}\text{C}$  evidence. *Science*, 256, 74–79. <https://doi.org/10.1126/science.256.5053.74>
- R Core Team. (2019). *R: A language and environment for statistical computing*. R Foundation for Statistical Computing, Vienna, Austria. Retrieved from <https://www.R-project.org/>
- Rooney, N., McCann, K., Gellner, G., & Moore, J. C. (2006). Structural asymmetry and the stability of diverse food webs. *Nature*, 442, 265–269. <https://doi.org/10.1038/nature04887>
- Sherwood, O. A., Guilderson, T. P., Batista, F. C., Schiff, J. T., & McCarthy, M. D. (2014). Increasing subtropical North Pacific Ocean nitrogen fixation since the Little Ice Age. *Nature*, 505, 78–81. <https://doi.org/10.1038/nature12784>
- Sherwood, O. A., Lehmann, M. F., Schubert, C. J., Scott, D. B., & McCarthy, M. D. (2011). Nutrient regime shift in the western North Atlantic indicated by compound-specific  $\delta^{15}\text{N}$  of deep-sea gorgonian corals. *Proceedings of the National Academy of Sciences of the United States of America*, 108, 1011–1015. <https://doi.org/10.1073/pnas.1004904108>



- Smith, S. L., Henrichs, S. M., & Rho, T. (2002). Stable C and N isotopic composition of sinking particles and zooplankton over the south-eastern Bering Sea shelf. *Deep Sea Research Part II: Topical Studies in Oceanography*, 49, 6031–6050. [https://doi.org/10.1016/S0967-0645\(02\)00332-6](https://doi.org/10.1016/S0967-0645(02)00332-6)
- Stabeno, P. J., Bond, N. A., & Salo, S. A. (2007). On the recent warming of the southeastern Bering Sea shelf. *Deep Sea Research Part II: Topical Studies in Oceanography*, 54, 2599–2618. <https://doi.org/10.1016/j.dsr2.2007.08.023>
- Stachura, M. M., Essington, T. E., Mantua, N. J., Hollowed, A. B., Haltuch, M. A., Spencer, P. D., Branch, T. A., & Doyle, M. J. (2014). Linking Northeast Pacific recruitment synchrony to environmental variability. *Fisheries Oceanography*, 23, 389–408. <https://doi.org/10.1111/fog.12066>
- Stan Development Team. (2019). RStan: The R interface to Stan. R Package Version, 2(19), 2. Retrieved from <http://mc-stan.org/>
- Strom, S. L., Brady, O. M., Macri, E. L., & Mordy, C. W. (2006). Cross-shelf gradients in phytoplankton community structure, nutrient utilization, and growth rate in the coastal Gulf of Alaska. *Marine Ecology Progress Series*, 328, 75–92.
- Tagliabu, A., & Bopp, L. (2008). Towards understanding global variability in ocean carbon-13. *Global Biogeochemical Cycles*, 22, GB1025. <https://doi.org/10.1029/2007GB003037>
- van Klinken, G. J. (1999). Bone collagen quality indicators for palaeo-dietary and radiocarbon measurements. *Journal of Archaeological Science*, 26, 687–695. <https://doi.org/10.1006/jasc.1998.0385>
- Vecchi, G. A., & Wittenberg, A. T. (2010). El Niño and our future climate: Where do we stand? *Wires Climate Change*, 1, 260–270. <https://doi.org/10.1002/wcc.33>
- Vehtari, A., Gelman, A., & Gabry, J. (2017). Practical Bayesian model evaluation using leave-one-out cross-validation and WAIC. *Statistics and Computing*, 27, 1413–1432. <https://doi.org/10.1007/s11222-016-9696-4>
- Vokshoori, N. L., & McCarthy, M. D. (2014). Compound-specific  $\delta^{15}\text{N}$  amino acid measurement in littoral mussels in the California upwelling ecosystem: A new approach to generating baseline  $\delta^{15}\text{N}$  isoscapes for coastal ecosystems. *PLoS One*, 9, e98087. <https://doi.org/10.1371/journal.pone.0098087>
- Waite, J. N., & Mueter, F. J. (2013). Spatial and temporal variability of chlorophyll-*a* concentrations in the coastal Gulf of Alaska, 1998–2011, using cloud-free reconstructions of SeaWiFS and MODIS-Aqua data. *Progress in Oceanography*, 116, 179–192. <https://doi.org/10.1016/j.pocean.2013.07.006>
- Ware, D. M., & Thomson, R. E. (2005). Bottom-up ecosystem trophic dynamics determine fish production in the Northeast Pacific. *Science*, 308, 1280–1284. <https://doi.org/10.1126/science.1109049>
- Whitney, N. M., Johnson, B. J., Dostie, P. T., Luzier, K., & Wanamaker, A. D. (2019). Paired bulk organic and individual amino acid  $\delta^{15}\text{N}$  analyses of bivalve shell peristracum: A paleoceanographic proxy for water source variability and nitrogen cycling processes. *Geochimica Et Cosmochimica Acta*, 254, 67–85. <https://doi.org/10.1016/j.gca.2019.03.019>
- Williams, B., Risk, M., Stone, R., Sinclair, D., & Ghaleb, B. (2007). Oceanographic changes in the North Pacific Ocean over the past century recorded in deep-water gorgonian corals. *Marine Ecology Progress Series*, 335, 85–94. <https://doi.org/10.3354/meps335085>
- Wu, J., Clavert, S. E., & Wong, C. S. (1997). Nitrogen isotope variations in the subarctic northeast Pacific: Relationships to nitrate utilization and trophic structure. *Deep Sea Research Part 1: Oceanographic Research Papers*, 44, 287–314. [https://doi.org/10.1016/S0967-0637\(96\)00099-4](https://doi.org/10.1016/S0967-0637(96)00099-4)
- Zuur, A. F., Tuck, I. D., & Bailey, N. (2003). Dynamic factor analyses to estimate common trends in fisheries time series. *Canadian Journal of Fisheries and Aquatic Science*, 60, 542–552. <https://doi.org/10.1139/f03-030>

## SUPPORTING INFORMATION

Additional supporting information may be found online in the Supporting Information section.

**How to cite this article:** Feddern ML, Holtgrieve GW, Ward EJ. Stable isotope signatures in historic harbor seal bone link food web-assimilated carbon and nitrogen resources to a century of environmental change. *Glob Change Biol*. 2021;27:2328–2342. <https://doi.org/10.1111/gcb.15551>